

**Temperature effects in luminescence of associated oxygen-carbon pairs
in hexagonal boron nitride under direct optical excitation within 7-1100 K range**

A.S. Vokhmintsev, I.A. Weinstein

NANOTECH Centre, Ural Federal University, 19 Mira street, Ekaterinburg 620002, Russia

a.s.vokhmintsev@urfu.ru, i.a.weinstein@urfu.ru

We have studied the temperature dependencies of the photoluminescence (PL) intensity of 4.1 eV in microcrystalline powder of hexagonal boron nitride in the range of 7-1100 K. The results obtained have been analyzed within the band model of energy levels of associated donor-acceptor pairs based on impurity ($O_N C_N$) complexes. Luminescence enhancement processes at $T < 200$ K and two independent channels of external thermal activation quenching are typical of the observable luminescence mechanisms under direct (4.26 eV) excitations of the samples. It has been shown that, at $T > 220$ K, when directly excited, the samples diminish the PL intensity because of the processes of thermal ionization of the donor level of the O_N -center (122 meV) and the deep acceptor level of the C_N -center (1420 meV) as parts of the ($O_N C_N$)-complex. The temperature enhancement region with an activation energy of 15 meV is due to the decay of a bound Wannier-Mott exciton followed by transfer of excitation to the associated donor-acceptor pair.

Currently, much attention is being paid to the directed synthesis method, treatment and alloying of hexagonal boron nitride (h-BN) to create van der Waals heterostructures with desired properties.¹⁻⁴ This may be base for developing promising functional media for applications in nano- and optoelectronics.^{5,6} In particular, owing to bandgap engineering technologies, single-photon emitters (SPEs) can be realized in h-BN, which operate in the room temperature range and exhibit zero-phonon-line energies (E_{ZPL}) in the visible (Vis) and ultraviolet (UV) spectral regions.⁷⁻¹² The SPE luminescence in the Vis region⁷⁻¹¹ is associated with complexes of point defects such as a nitrogen atom in the boron position with an anti-site nitrogen vacancy ($N_B V_N$)^{9,10} and a boron vacancy with two oxygen atoms on the surface ($V_B O_2$).⁸

At the same time, upon treated with ultrasound, commercial h-BN micropowders show a bright emission of SPE in the UV region with an energy of $E_{ZPL} = 4.1$ eV and several phonon replicas separated by an energy of ≈ 0.18 eV.¹² It is known that the indicated luminescence in the as-grown h-BN samples with impurities of carbon and oxygen is observed under subband and band-to-band excitation, and proceeds by the donor-acceptor mechanism.¹³⁻¹⁶ Moreover, the subband excitation can be regarded as direct optical one of the ($O_N C_N$)-complex, which leads to an inter-impurity electronic transitions¹⁶ and is characterized by the fast kinetics of luminescence

decay (≈ 1 ns).^{15,17} Earlier studies related $E_{ZPL}=4.1$ eV energy emission with radiative recombination of either “band – C_N-center” (carbon atom in the nitrogen position)^{18,19} or “an unknown shallow donor – C_N-center”.¹⁵ The former is characterized by a deep acceptor level in the bandgap at a distance of 1.2-2.4 eV from the valence band top.^{14,18-21} Later, the luminescence at hand was attributed to donor-acceptor recombination by a complex of associated (located at the minimum possible distance) point defects such as a nitrogen vacancy with a carbon atom in the nitrogen position (V_NC_N)^{14,22}, oxygen and carbon atoms in nitrogen positions (O_NC_N)^{16,23}, and carbon atoms in boron and nitrogen positions (C_BC_N).^{24,25} Besides, the Ref. 26 showed that annealing of an h-BN micropowder in an O₂ atmosphere at a temperature of 900 °C for 2 h results in an increase in both the oxygen content from 0.25 to 0.40 wt. % and the intensity of cathodoluminescence in the 320 nm (3.9 eV) band by almost 4 times as compared to the initial sample. However, no correlation between the impurity (carbon and oxygen) concentration and $E_{ZPL}\approx 4.1$ eV emission intensity was found when comparing photoluminescence measurements and quantitative trace impurity analysis of variously heat-treated h-BN samples.²⁷ From the foregoing, it is clear that identifying the nature of the excited state of an optically active complex that luminesces with an energy of $E_{ZPL}=4.1$ eV and the role of oxygen in its formation faces some contradictions.

The objective of the present work is to investigate the temperature behavior of photoluminescence (PL) in the range of 7-1100 K for direct optical excitations of 4.1 eV luminescence centers in h-BN micropowder. The observable experimental regularities are discussed within the band model for energy levels structure of associated donor-acceptor pair (DAP) based on an impurity (O_NC_N)-complex.

The studied h-BN micropowder was synthesized under conditions of N deficiency, and C (2.9 ± 0.1 at.%) and O (0.6 ± 0.1 at.%) were the main impurities.^{16,20} The PL intensity was measured in the range of 300-1100 K using a Perkin Elmer LS55 spectrometer equipped with a compact high-temperature attachment.^{28,29} For taking the measurements in the range of 7-335 K, a Janis CCS-100/204N closed-cycle helium cryostat was used, combined with the recording channel of the Perkin Elmer LS55 spectrometer.¹⁶ To exclude the possible influence of the thermally stimulated luminescence signal, the PL temperature dependencies were measured in cooling regime.³⁰ The cooling rates amounted to 0.1 and 1.0 K/s in the ranges of 7-335 and 300-1100 K, respectively. The emission at 3.90 eV was recorded under 4.26 eV excitation. Figure 1 presents PL spectra for the studied DAPs with $E_{ZPL} = 4.1$ eV. The spectra exhibit obvious vibrational structure with phonon replicas of $\hbar\omega=174$ and 164 meV in the PL emission and excitation, respectively. Analyzed 3.90 and 4.26 eV bands correspond to the first phonon replicas

in the PL emission and excitation, respectively (see Figure 1). This fact is consistent with the known experiments.^{15,16,25,27}

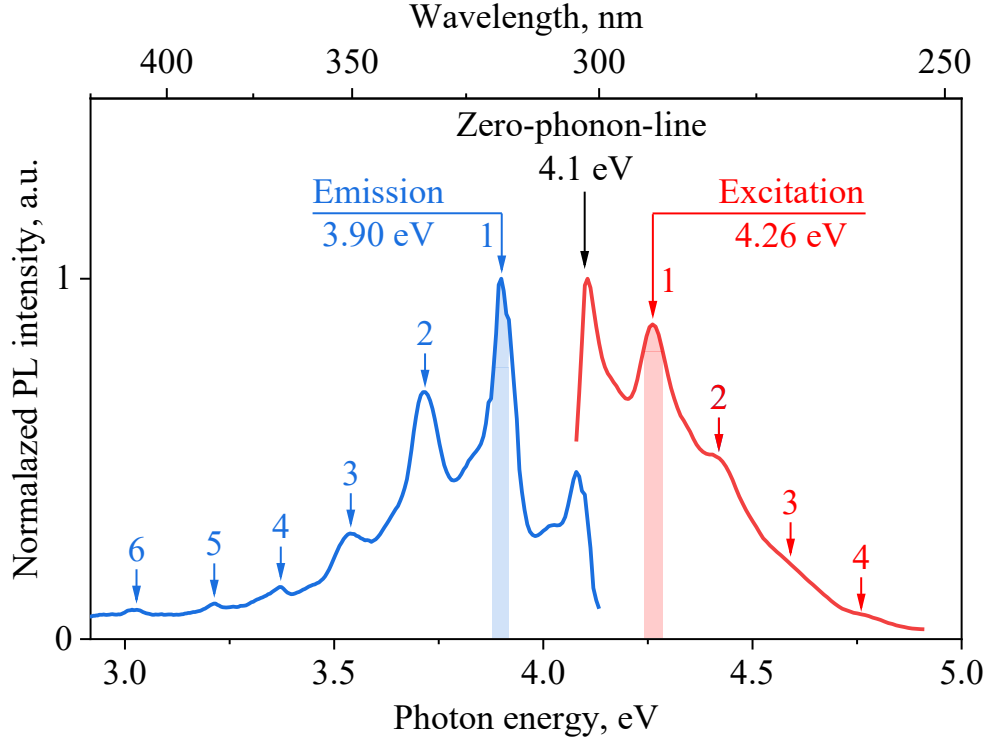


Figure 1. Normalized excitation and emission PL spectra of (O_NC_N)-complex measured at room temperature. Arrows show replicas positions caused by emission and excitation processes with participating the phonons with energies of $\hbar\omega = 174$ and 164 meV, respectively.

Figure 2 presents the $I(T)$ temperature dependence measured for the PL intensity in the 3.90 eV of the h-BN powder investigated. As can be seen from the experimental curves, the luminescence intensity increases in the range of 7 - 220 K and reaches its maximum (I_{max}) in the region $T_{max}=220$ - 260 K. When heated to $T>T_{max}$ (≈ 1100 K) and excited in the band of 4.26 eV the sample loses its PL intensity up to background values. Thus, the measured dependencies of the PL response in studied h-BN are characterized by two regions with different temperature behavior, but namely, luminescence enhancement (“negative” temperature quenching) is observed at $T<T_{max}$ and the conventional thermal quenching of PL is characteristic of the region $T>T_{max}$. The dependence on Figure 2, insert, highlights two linear segments intersected at point of $(kT)^{-1}\approx 12.2$ eV⁻¹ ($T\approx 950$ K) in the region $(kT)^{-1}<40$ eV⁻¹ ($T>290$ K). In this case, it can be claimed that there are at least two non-radiative thermally activated quenching channels with energies E_{Q1} and E_{Q2} in the temperature range at hand.

Considering the foregoing, we conducted a further quantitative analysis of the $I(T)$ experimental dependencies within the modified Mott relation.^{21,31} The latter contains

independent efficiencies for two non-radiative relaxation channels (denominator) and the efficiency of the PL enhancement process (numerator)³²:

$$I(T) = I_0 \frac{1 + p' \exp\left(-\frac{E'}{kT}\right)}{1 + p_1 \exp\left(-\frac{E_{Q1}}{kT}\right) + p_2 \exp\left(-\frac{E_{Q2}}{kT}\right)} \quad (1)$$

where I_0 is the PL intensity at $T = 0$ K, a.u.; p' is the dimensionless pre-exponential factor of the PL enhancement process; E' is the activation energy of the luminescence enhancement process, eV; k is the Boltzmann constant, eV/K; T is the temperature, K; p_1 and p_2 are the dimensionless pre-exponential factors of temperature quenching processes; E_{Q1} and E_{Q2} are activation energies of luminescence quenching processes, eV.

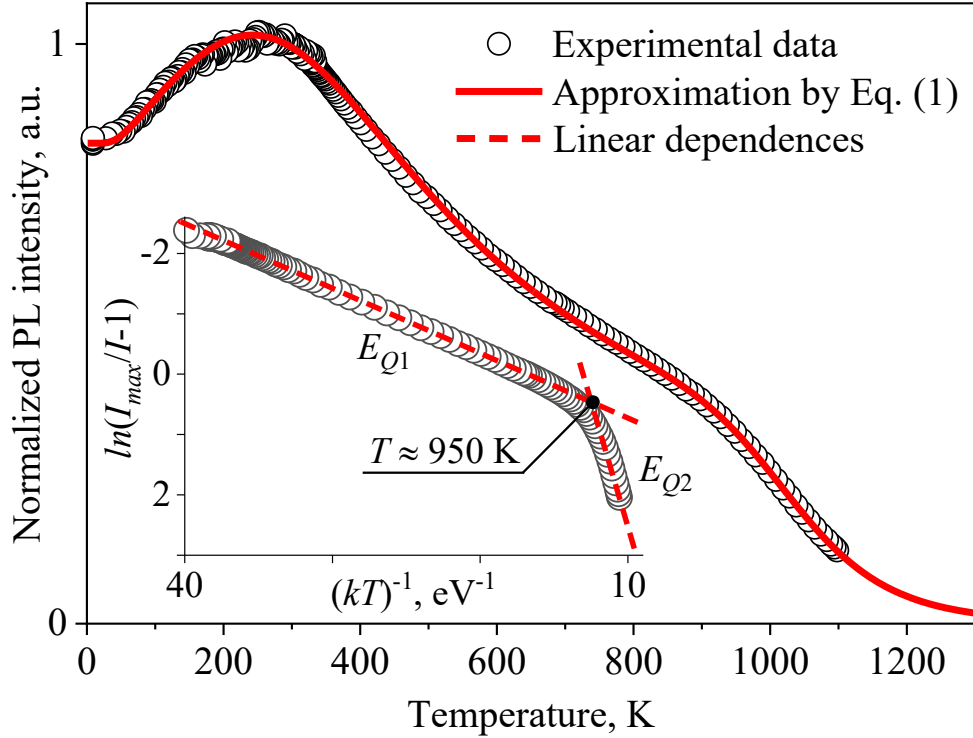


Figure 2. Normalized temperature dependencies of the PL intensity in the band of 3.90 eV at 4.26 eV excitation. Insert shows experimental data in Arrhenius coordinates.

The solid lines in Figure 2 display approximations of experimental data according to Eq. (1) with determination coefficients $R^2 > 0.998$. The following approximation parameters are obtained: $I_0 = 0.829 \pm 0.001$ a.u., $p' = 0.53 \pm 0.01$, $E' = 15 \pm 1$ meV, $p_1 = 9.0 \pm 0.1$, $E_{Q1} = 122 \pm 1$ meV, $p_2 = (2.0 \pm 0.2) \cdot 10^7$, $E_{Q2} = 1420 \pm 10$ meV.

Figure 3 illustrates a band scheme for PL processes at 3.90 eV (② transition) for the studied defect complex at excitation of the h-BN samples in at 4.26 eV (① transition). Upon absorbing a light quantum with an energy of 4.26 eV (① transition), an electron e passes from the C_N -center level to the O_N -center level, generating e and h localized at the levels of the O_N - and C_N -centers, respectively (see Figure 3(b)). This, in turn, leads to a change in the local charge of each of the impurities and their transition to a neutral state. According to the results calculated in Ref. 33, it can be argued that the unpaired electron of the P_z non-hybridized atomic orbital of the carbon atom involves in PL under study.

During selective excitation of the ($O_N C_N$)-complex, the quenching mechanism is produced by two independent channels (③ and ④ transitions) with activation energies of $E_{Q1}=122$ meV and $E_{Q2}=1420$ meV, respectively. The value of E_{Q2} is consistent with the ionization energy of the deep acceptor level of the C_N -center in h-BN, equal to 1.2-2.4 eV.^{14,18-21} It can be assumed that the value of E_{Q1} corresponds to the shallow donor level of the O_N -center in the impurity complex under study. During direct optical excitation, the ionization of O_N -centers dominates due to the thermally activated transition of an electron from the first vibrational level to the conduction band.

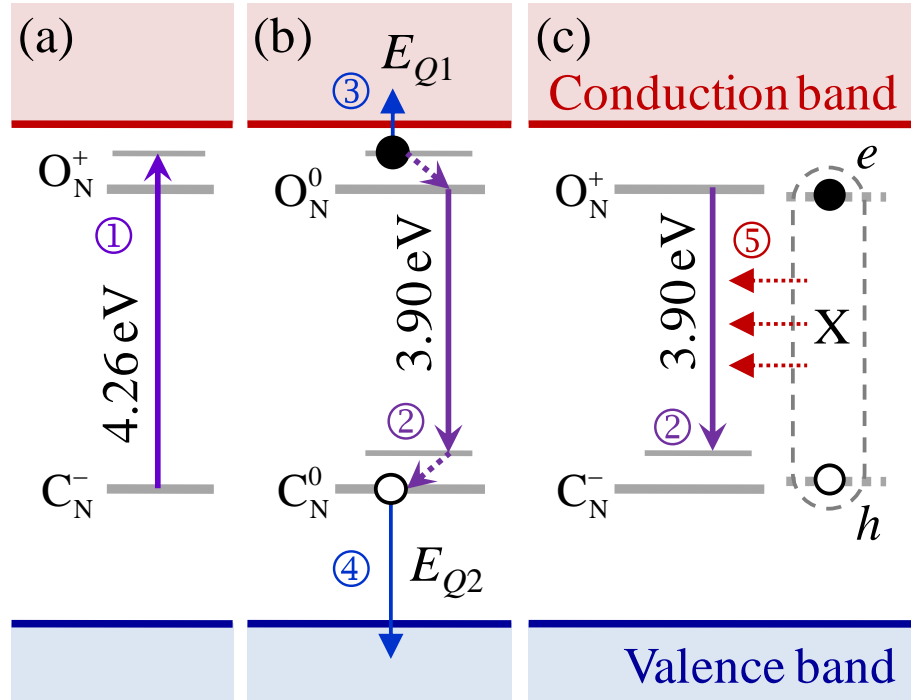
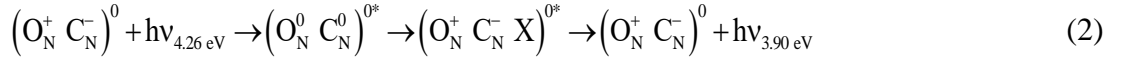


Figure 3. A band diagram of luminescence processes for an ($O_N C_N$)-complex under direct optical excitation: (a) excitation; (b) emission and external thermal quenching of PL; (c) emission and thermal enhancement of the photoluminescence.

The observable thermally activated enhancement of the PL (see Figure 2) with an energy $E'=15$ meV may be due to the formation of an exciton bound to the defect. A system consisting of closely spaced (associated) neutral donor O_N^0 and acceptor C_N^0 can be interpreted as an exciton bound with DAP (X-DAP), see Figure 3(c).³⁴ In this case, the X-DAP complex consists of four point-charges. Two of them are motionless: a donor ion O_N^+ and an acceptor ion C_N^- . The other two point-charges (e and h) are localized in the region of the O_N^- and C_N^- -centers, respectively. Consequently, for the $(O_N C_N)$ -complex excited in the 4.26 eV band, we can write down:



According to Ref. 35, the binding energy of an exciton with an neutral impurity complex (E_X) satisfies the condition:

$$0.055 E_i < E_X < 0.33 E_i, \quad (3)$$

where E_i is the ionization energy of the impurity complex, eV.

The lower and upper limits in Eq. (3) correspond to the energy of electron detachment from a negatively charged hydrogen-like donor and dissociation of a hydrogen-like molecule, respectively. In our case, the binding energy between an exciton and the $(O_N C_N)$ -complex is determined by the lowest ionization energy of the oxygen impurity (O_N -center) $E_i^0 = E_{Q1} = 122$ meV. Using Eq. (3), we get $E_X = 7-40$ meV. It is seen that the activation energy of the luminescence enhancement process, equal to $E'=15$ meV, lies within the interval and matches the exciton binding energy.

In the model proposed for the X-DAP complex, the ground energy level of the bound exciton is located below the level of the excited state of the $(O_N C_N)$ complex by the energy $E_X \approx E' \approx 15$ meV. Thus, the PL enhancement process at low temperatures of $T < T_{max}$ can be due to the decay of the exciton (see Figure 3(c), \odot transition) followed by excitation transfer to DAP. Hence, in the region of low temperatures, the PL of the excitons under consideration should take place. This statement is confirmed by independent studies of h-BN samples, carried out by the macro- and micro-PL method with high spectral resolution at temperatures of 8 and 10 K, respectively.²⁵ In Ref. 25, a low-energy shoulder shifted relative to the 4.1 eV emission line by 10-20 meV was detected for the initial and carbon-doped h-BN samples. The authors of Ref. 25 did not discuss the nature of this shoulder and the oxygen content in the samples studied.

However, according to the results of the present research work, the observable spectral shoulder can be associated with impurity-bound excitons.

Within the hydrogen-like approximation, let us evaluate the most probable radii (r) of the orbits for charge carriers localized near impurity ions³⁵:

$$r = \frac{a_B R_y}{\varepsilon E_i}, \quad (4)$$

where $a_B=0.53 \text{ \AA}$ is the Bohr radius; $R_y=13.6 \text{ eV}$ is the Rydberg constant; $\varepsilon=3.5$ is the relative dielectric constant for h-BN.³⁶ The specified value is equal to $r_O=18.4 \text{ \AA}$ for e at the O_N -center and $r_C=1.5 \text{ \AA}$ for h in the region of the C_N -center. The minimum distance between e and h in question exceeding the interatomic distances in the h-BN crystal lattice, it can be claimed that, at $T < T_{max}$, it is a Wannier-Mott exciton that is probably expected to be localized on the impurity ($O_N C_N$)-complex. The assumption made above is consistent with the PL enhancement experimentally recorded (see Figure 2) in the cryogenic temperature range for the h-BN samples examined.

Earlier, the research work proposed the Wannier-Mott exciton model to discuss the results of experimental studies of the optical properties of pure h-BN single crystals.³⁷ Later, a lot of articles have also reported on luminescence bands near the edge of the bandgap in h-BN involving impurity-bound (or trapped) excitons.^{15,25,38-41}

Let us look into the process of selective excitation of the ($O_N C_N$)-complex using the model proposed and describe, step by step, the transition of e between the C and O impurity levels. First, when thus excited, the C_N -center goes into a neutral state. In other words, h localized on it emerges: $C_N^- + h\nu_{4.28 \text{ eV}} \rightarrow C_N^0 + e$. Simultaneously, a positively charged O_N -center resides at the smallest possible distance of $R \approx 2.5 \text{ \AA}$ between O and C in the associated ($O_N C_N$)-pair in the nearest N positions. Due to the Coulomb repulsion, the binding energy of h formed at the C_N -center increases by the value of $\frac{q^2}{\varepsilon R} \approx 1.64 \text{ eV}$, where q is the charge of an electron. Next, excited e is localized at the O_N -center in the presence of an already neutral C_N -center and the impurity O passes into a neutral state: $C_N^0 + e + O_N^+ \rightarrow C_N^0 + O_N^0$. When the donor and acceptor are closely spaced to each other, the van der Waals force begins to act between them. In this case, the binding energy of e localized at the O_N -center grows by the value of $W(R)$. We write down the expression for the radiation energy upon recombination of DAP^{34,35}:

$$\begin{aligned}
E_{em} &= E_g - E_i^C + \frac{q^2}{\epsilon R} - E_i^O + W(R) = \\
&= E_g - \left(E_i^C - \frac{q^2}{\epsilon R} \right) - (E_i^O - W(R))
\end{aligned} \tag{5}$$

where E_g is the bandgap h-BN; E_i^O and E_i^C are the positions of the energy levels of isolated O_N and C_N -centers, respectively.

The Eq. (5) implies that the association of the O_N - and C_N -centers causes a shift in the position of their energy levels to the bottom of conduction band and the top of valence band, respectively. In the case of external mechanisms of temperature quenching of the PL studied, the

ionization energy of the isolated C_N -center is equal to $E_i^C = E_{Q2} + \frac{e^2}{\epsilon R} = 1.42 + 1.64 = 3.06$ eV. The

value obtained is in agreement with the position of the 3.19 eV energy level relative to the valence band top for an isolated C_N -center in h-BN.⁴² The calculation by the method of density functional theory within the generalized Kohn-Sham scheme also confirms the above assertion.⁴²

Meanwhile, according to the Eq. (5), the $W(R)$ van der Waals summand is necessary to know to compute the ionization energy of the independent O_N -center. An analysis of the calculation works showed that the binding energy between two layers in h-BN varies in the range of 55-152 meV.^{43,44} Suppose that, for the $(O_N C_N)$ -complex at hand, the van der Waals summand takes similar values, i.e., $W(R) = 55-152$ meV. In this case, taking into account the quenching energy and the position of the first phonon replica for DAP donor level of the DAP ($E_{Q1} + \hbar\omega = 122 + 164$ meV), the ionization energy of the independent O_N -center is $E_i^O = 341-438$ meV. The above value is consistent with an activation energy of 300-500 meV for electron trap based on O_N -center.^{18,45}

In summary, the temperature dependencies of photoluminescence have been measured in the 3.90 eV band in the range of 7-1100 K under direct (4.26 eV) excitation of h-BN micropowder samples with C and O impurities. A region of PL enhancement in the temperature range of $T < 200$ K was found. The obtained experimental data were analyzed within a model with one PL enhancement channel and two independent channels of external temperature quenching. The corresponding activation energies of the investigated processes are estimated. It is shown that with quenching of PL with energies of 122 and 1420 meV is due, respectively, to the thermal ionization of a shallow donor O_N -level and deep acceptor C_N -level as parts of the impurity $(O_N C_N)$ -complex under study. Within the hydrogen-like approximation, the most probable radii of the orbits of localization of electrons and holes by the O and C impurity ions were calculated. They amount to 18.4 and 1.5 Å, respectively. The PL enhancement in the

temperature dependence is assumed to be contributed by the decay of Wannier-Mott excitons, which are bound with the impurity complex in question and have a binding energy of 15 meV.

Acknowledgments

The work was supported by Act 211 Government of the Russian Federation, contract № 02. A03.21.0006 and by Minobrnauki research project.

References

-
- ¹Novoselov K.S., Mishchenko A., Carvalho A., Castro Neto A.H. (2016) 2D materials and van der Waals heterostructures // *Science*, Volume 353, Issue 6298, Article number aac9439, <https://doi.org/10.1126/science.aac9439>
- ²Zomer P.J., Guimarães M.H.D., Brant J.C., Tombros N., Van Wees B.J. (2014) Fast pick up technique for high quality heterostructures of bilayer graphene and hexagonal boron nitride // *Applied Physics Letters*, Volume 105, Issue 1, Article number 013101, <https://doi.org/10.1063/1.4886096>
- ³Kamalakar M.V., Dankert A., Bergsten J., Ive T., Dash S.P. (2014) Spintronics with graphene-hexagonal boron nitride van der Waals heterostructures // *Applied Physics Letters*, Volume 105, Issue 21, Article number 212405, <https://doi.org/10.1063/1.4902814>
- ⁴Watanabe K., Taniguchi T. (2019) Far-UV photoluminescence microscope for impurity domain in hexagonal-boron-nitride single crystals by high-pressure, high-temperature synthesis // *npj 2D Materials and Applications*, Volume 3, Issue 1, Article number 40, <https://doi.org/10.1038/s41699-019-0124-4>
- ⁵Dean C.R., Young A.F., Meric I., Lee C., Wang L., Sorgenfrei S., Watanabe K., Taniguchi T., Kim P., Shepard K.L., Hone J. (2010) Boron nitride substrates for high-quality graphene electronics // *Nature Nanotechnology*, Volume 5, Issue 10, Pages 722-726, <https://doi.org/10.1038/nnano.2010.172>
- ⁶Dahal R., Li J., Majety S., Pantha B.N., Cao X.K., Lin J.Y., Jiang H.X. (2011) Epitaxially grown semiconducting hexagonal boron nitride as a deep ultraviolet photonic material // *Applied Physics Letters*, Volume 98, Issue 21, Article number 211110, <https://doi.org/10.1063/1.3593958>
- ⁷Jungwirth N.R., Fuchs G.D. (2017) Optical Absorption and Emission Mechanisms of Single Defects in Hexagonal Boron Nitride // *Physical Review Letters*, Volume 119, Issue 5, Article number 057401, <https://doi.org/10.1103/PhysRevLett.119.057401>
- ⁸Xu Z.-Q., Elbadawi C., Tran T.T., Kianinia M., Li X., Liu D., Hoffman T.B., Nguyen M., Kim S., Edgar J.H., Wu X., Song L., Ali S., Ford M., Toth M., Aharonovich I. (2018) Single photon

-
- emission from plasma treated 2D hexagonal boron nitride // *Nanoscale*, Volume 10, Issue 17, Pages 7957-7965, <https://doi.org/10.1039/c7nr08222c>
- ⁹Grosso G., Moon H., Lienhard B., Ali S., Efetov D.K., Furchi M.M., Jarillo-Herrero P., Ford M.J., Aharonovich I., Englund D. (2017) Tunable and high-purity room temperature single-photon emission from atomic defects in hexagonal boron nitride // *Nature Communications*, Volume 8, Issue 1, Article number 705, <https://doi.org/10.1038/s41467-017-00810-2>
- ¹⁰Tran T.T., Bray K., Ford M.J., Toth M., Aharonovich I. (2016) Quantum emission from hexagonal boron nitride monolayers // *Nature Nanotechnology*, Volume 11, Issue 1, Pages 37-41, <https://doi.org/10.1038/nnano.2015.242>
- ¹¹Tran T.T., Elbadawi C., Totonjian D., Lobo C.J., Grosso G., Moon H., Englund D.R., Ford M.J., Aharonovich I., Toth M. (2016) Robust Multicolor Single Photon Emission from Point Defects in Hexagonal Boron Nitride // *ACS Nano*, Volume 10, Issue 8, Pages 7331-7338, <https://doi.org/10.1021/acsnano.6b03602>
- ¹²Bourrellier R., Meuret S., Tararan A., Stéphan O., Kociak M., Tizei L.H.G., Zobelli A. (2016) Bright UV single photon emission at point defects in h-BN // *Nano Letters*, Volume 16, Issue 7, Pages 4317-4321, <https://doi.org/10.1021/acs.nanolett.6b01368>
- ¹³Taniguchi T., Watanabe K. (2007) Synthesis of high-purity boron nitride single crystals under high pressure by using Ba–BN solvent // *Journal of Crystal Growth*, Volume 303, Issue 2, Pages 525-529, <https://doi.org/10.1016/j.jcrysgro.2006.12.061>
- ¹⁴Du X.Z., Li J., Lin J.Y., Jiang H.X. (2015) The origin of deep-level impurity transitions in hexagonal boron nitride // *Applied Physics Letters*, Volume 106, Issue 2, Article number 021110, <https://doi.org/10.1063/1.4905908>
- ¹⁵Museur L., Feldbach E., Kanaev A. (2008) Defect-related photoluminescence of hexagonal boron nitride // *Physical Review B*, Volume 78, Issue 15, Article number 155204, <https://doi.org/10.1103/PhysRevB.78.155204>
- ¹⁶Vokhmintsev A., Weinstein I., Zamyatin D. (2019) Electron-phonon interactions in subband excited photoluminescence of hexagonal boron nitride // *Journal of Luminescence*, Volume 208, Pages 363-370, <https://doi.org/10.1016/j.jlumin.2018.12.036>
- ¹⁷Wu J., Han W.-Q., Walukiewicz W., Ager III J.W., Shan W., Haller E.E., Zettl A. (2004) Raman spectroscopy and time-resolved photoluminescence of BN and BxCyNz nanotubes // *Nano Letters*, Volume 4, Issue 4, Pages 647-650, <https://doi.org/10.1021/nl049862e>
- ¹⁸Katzir A., Suss J.T., Zunger A., Halperin A. (1975) Point defects in hexagonal boron nitride. I. EPR, thermoluminescence, and thermally-stimulated-current measurements // *Physical Review B*, Volume 11, Issue 6, Pages 2370-2377, <https://doi.org/10.1103/PhysRevB.11.2370>

-
- ¹⁹Uddin M.R., Li J., Lin J.Y., Jiang H.X. (2017) Probing carbon impurities in hexagonal boron nitride epilayers // *Applied Physics Letters*, Volume 110, Issue 18, Article number 182107, <https://doi.org/10.1063/1.4982647>
- ²⁰Vokhmintsev A.S., Minin M.G., Weinstein I.A. (2017) Estimation of thermoluminescence kinetic parameters in h-BN by different techniques // *Radiation Measurements*, Volume 106, Pages 55-60, <https://doi.org/10.1016/j.radmeas.2017.05.003>
- ²¹Vokhmintsev A.S., Weinstein I.A., Minin M.G., Shalyakin S.A. (2019) Thermally stimulated processes in the luminescence of carbon-related defects for h-BN micropowder // *Radiation Measurements*, Volume 124, Pages 35-39, <https://doi.org/10.1016/j.radmeas.2019.03.001>
- ²²Grenadier S.J., Maity A., Li J., Lin J.Y., Jiang H.X. (2018) Origin and roles of oxygen impurities in hexagonal boron nitride epilayers // *Applied Physics Letters*, Volume 112, Issue 16, Article number 162103, <https://doi.org/10.1063/1.5026291>
- ²³Shen Y., Yan H., Guo H., Long Y., Li W. (2020) Defect-rich hexagonal boron nitride for the simultaneous determination of 4-aminophenol and phenol // *Sensors and Actuators, B: Chemical*, Volume 303, Article number 127248, <https://doi.org/10.1016/j.snb.2019.127248>
- ²⁴MacKoit-Sinkevičiene M., MacIaszek M. Van De Walle C.G., Alkauskas A. (2019) Carbon dimer defect as a source of the 4.1 eV luminescence in hexagonal boron nitride // *Applied Physics Letters*, Volume 115, Issue 21, Article number 212101, <https://doi.org/10.1063/1.5124153>
- ²⁵Pelini T., Elias C., Page R., Xue L., Liu S., Li J., Edgar J.H., Dréau A., Jacques V., Valvin P., Gil B., Cassaboiss G. (2019) Shallow and deep levels in carbon-doped hexagonal boron nitride crystals // *Physical Review Materials*, Volume 3, Issue 9, Article number 094001, <https://doi.org/10.1103/PhysRevMaterials.3.094001>
- ²⁶Hara K., Liu X., Yamauchi M., Kawanishi Y., Kominami H., Nakanishi Y. (2011) Effects of annealing on 320 nm cathodoluminescence from hexagonal boron nitride powders // *Physica Status Solidi (C)*, Volume 8, Issue 7-8, Pages 2509-2511, <https://doi.org/10.1002/pssc.201001159>
- ²⁷Tsushima E., Tsujimura T., Uchino T. (2018) Enhancement of the deep-level emission and its chemical origin in hexagonal boron nitride // *Applied Physics Letters*, Volume 113, Issue 3, Article number 031903, <https://doi.org/10.1063/1.5038168>
- ²⁸Vokhmintsev A.S., Minin M.G., Henaish A.M.A., Weinstein I.A. (2015) Spectrally resolved thermoluminescence measurements in fluorescence spectrometer // *Measurement*, Volume 66, Pages 90-94, <https://doi.org/10.1016/j.measurement.2015.01.012>
- ²⁹Vokhmintsev A.S., Minin M.G., Chaykin D.V., Weinstein I.A. (2014) A high-temperature accessory for measurements of the spectral characteristics of thermoluminescence //

-
- Instruments and Experimental Techniques, Volume 57, Issue 3, Pages 369-373, <https://doi.org/10.1134/S0020441214020328>
- ³⁰Weinstein I.A., Vokhmintsev A.S., Kortov V.S. (2006) Thermal quenching of 3.0-eV photoluminescence in α -Al₂O₃ single crystals // Technical Physics Letters, Volume 32, Issue 1, Pages 58-60, <https://doi.org/10.1134/S1063785006010196>
- ³¹Henaish A.M.A., Vokhmintsev A.S., Weinstein I.A. (2016) Two-level quenching of photoluminescence in hexagonal boron nitride micropowder // AIP Conference Proceedings, Volume 1717, Article number 4943473, <https://doi.org/10.1063/1.4943473>
- ³²Shibata H. (1998) Negative thermal quenching curves in photoluminescence of solids // Japanese Journal of Applied Physics, Volume 37, Issue 2, Pages 550-553, <https://iopscience.iop.org/article/10.1143/JJAP.37.550/pdf>
- ³³Huang B., Lee H. (2012) Defect and impurity properties of hexagonal boron nitride: A first-principles calculation // Physical Review B, Volume 86, Issue 24, Article number 245406, <https://doi.org/10.1103/PhysRevB.86.245406>
- ³⁴H. Barry Bebb, E.W. Williams (1972) Photoluminescence I: theory, in: R.K. Willardson, A.C. Beer (Eds.), Semiconductors and Semimetals, Vol. 8: Transport and Optical Phenomena, Academic Press, New York and London, pp. 181–320 (Transport and Optical Phenomena).
- ³⁵I. Pelant, J. Valenta (2012) Luminescence Spectroscopy of Semiconductors, Oxford University Press, New York, <https://doi.org/10.1093/acprof:oso/9780199588336.001.0001>
- ³⁶Sugino T., Tai T. (2000) Dielectric constant of boron nitride films synthesized by plasma-assisted chemical vapor deposition // Japanese journal of applied physics, Volume 39, Issue 11 A, Pages L1101-L1104, <https://iopscience.iop.org/article/10.1143/JJAP.39.L1101/pdf>
- ³⁷Watanabe K., Taniguchi T., Kanda H. (2004) Direct-bandgap properties and evidence for ultraviolet lasing of hexagonal boron nitride single crystal // Nature Materials, Volume 3, Issue 6, Pages 404-409, <https://doi.org/10.1038/nmat1134>
- ³⁸Watanabe K., Taniguchi T. (2009) Jahn-Teller effect on exciton states in hexagonal boron nitride single crystal // Physical Review B, Volume 79, Issue 19, Article number 193104, <https://doi.org/10.1103/PhysRevB.79.193104>
- ³⁹Doan T.C., Li J., Lin J.Y., Jiang H.X. (2016) Bandgap and exciton binding energies of hexagonal boron nitride probed by photocurrent excitation spectroscopy // Applied Physics Letters, Volume 109, Issue 12, Article number 102101, <https://doi.org/10.1063/1.4963128>
- ⁴⁰Du X.Z., Li J., Lin J.Y., Jiang H.X. (2016) The origins of near band-edge transitions in hexagonal boron nitride epilayers // Applied Physics Letters, Volume 108, Issue 5, Article number 052106, <https://doi.org/10.1063/1.4941540>

-
- ⁴¹Li J., Cao X.K., Hoffman T.B., Edgar J.H., Lin J.Y., Jiang H.X. (2016) Nature of exciton transitions in hexagonal boron nitride // *Applied Physics Letters*, Volume 108, Issue 12, Article number 122101, <https://doi.org/10.1063/1.4944696>
- ⁴²Weston L., Wickramaratne D., Mackoite M., Alkauskas A., Van De Walle C.G. (2018) Native point defects and impurities in hexagonal boron nitride // *Physical Review B*, Volume 97, Issue 21, Article number 214104, <https://doi.org/10.1103/PhysRevB.97.214104>
- ⁴³Hsing C.-R., Cheng C., Chou J.-P., Chang C.-M., Wei C.-M. Van der Waals interaction in a boron nitride bilayer // *New Journal of Physics*, Volume 16, 7 November 2014, Article number 13015, <https://doi.org/10.1088/1367-2630/16/11/113015>
- ⁴⁴Hummel F., Gruber T., Grüneis A. (2016) A many-electron perturbation theory study of the hexagonal boron nitride bilayer system // *European Physical Journal B*, Volume 89, Issue 11, Article number 235, <https://doi.org/10.1140/epjb/e2016-70177-4>
- ⁴⁵Ohtani S., Yano T., Kondo S., Kohno Y., Tomita Y., Maeda Y., Kobayashi K. (2013) Electron emission from h-BN films codoped with Mg and O atoms // *Thin Solid Films*, Volume 546, Pages 53-57, <https://doi.org/10.1016/j.tsf.2013.05.027>